Molecular Level Models for CO_2 Sorption in Nanopores

Aleksey Vishnyakov, Peter I. Ravikovitch, and Alexander V. Neimark*

TRI/Princeton, 601 Prospect Avenue, Princeton, New Jersey 08542-0625

Received June 8, 1999. In Final Form: July 27, 1999

Adsorption of carbon dioxide in slit-shaped carbon micropores at 273 K has been studied by means of the grand canonical Monte Carlo (GCMC) simulations and the nonlocal density functional theory (NLDFT). Three molecular models of CO_2 have been used. Long-run GCMC simulations were performed with the three-center model of Harris and Yung (*J. Phys. Chem.* **1995**, *99*, 12021). For NLDFT calculations, we developed an effective Lennard-Jones (LJ) model. GCMC simulations of the effective LJ model of CO_2 have been performed for comparison. For each model used, parameters of intermolecular potentials have been determined and validated against two-phase bulk equilibrium data and experimental adsorption isotherms on graphite at 273 and 195 K. In the range of pore widths from 3 to 15 Å, the NLDFT isotherms of CO_2 adsorption are overall in a satisfactory agreement with the GCMC isotherms generated using the three-center model. Some deviations have been observed between 6.5 and 8.5 Å, where the adsorbate undergoes a transition from a single-layer to a two-layer structure. The models developed are recommended for studying carbon dioxide adsorption in microporous adsorbents and also for calculating pore size distributions in carbonaceous materials and soil particles. The NLDFT model has the advantage of being much less computationally demanding, whereas the three-center GCMC model serves as a benchmark for quantitative estimates and can be used for studying CO_2 sorption at ambient conditions close to the critical temperature.

Introduction

Intensive studies of carbon dioxide sorption by nanoporous materials are motivated mainly by the urgent practical problem of the removal of CO_2 from various environments. Activated carbons and carbon fibers are capable of adsorbing rapidly substantial amounts of CO_2 at ambient temperatures and atmospheric pressures and, therefore, are efficient for CO_2 sorption. For the same reasons, CO_2 sorption at ambient temperatures and pressures is a promising technique for characterization of nanoporosity in carbonaceous materials, such as active carbons,[2] coals, and soil organic particles containing natural organic matter, for example, humic substances.[3,4] Traditional methods of quantitative description of CO_2 sorption in microporous sorbents are based on empirical Dubinin's theory.[5] However, there are controversial opinions on the real state of CO_2 in carbon micropores.[6−8] On the basis of experimental studies, some authors supposed that at ambient temperatures CO_2 would achieve the density comparable with the bulk liquid density only in the narrowest pores, in which the potential fields from the opposite walls overlap.[9] The others assumed that the pores of width of up to two molecular diameters would be filled at atmospheric pressure.[10] It was also suggested that CO_2 adsorbed in micropores is able to form a liquidlike phase in wider pores also.[11]

Different modifications of Dubinin's theory have been proposed in the literature. An alternative approach is based on molecular modeling of interactions of CO_2 with carbonaceous surfaces by means of grand canonical Monte Carlo (GCMC) simulations or density functional theory (DFT) calculations. Several GCMC studies of CO_2 sorption on graphite surfaces and slit-shaped pores have been reported. Bottani et al.[12,13] simulated CO_2 sorption on plane graphite surface at several temperatures between 195.5 and 273.2 K with parameters for solid−fluid interactions fitted to the experimental isotherm on Sterling graphite at 273 K within the Henry region. Cracknell et al.[14] and Nicholson and Gubbins[15] applied GCMC simulations to study separation of CH_4−CO_2 mixtures containing CO_2 by adsorption in ideal slit-shaped and cylindrical pores. A more sophisticated model of a slit-shaped pore with corrugated walls has been recently considered by Nicholson.[16] One-, two-, and three-center models were applied to study CO_2 adsorption in slit-shaped carbon pores by Gusev and Neimark.[17] Significant differences in adsorption isotherms generated using different models were found. Samios et al.[18] modeled CO_2 sorption at 195.5 K with application to characterization of active carbons. Ravikovitch et al. applied the nonlocal DFT (NLDFT) model for characterization of activated carbon fibers from CO_2 sorption at 273 K.[19]

* Author for correspondence.

(1) Harris, J. G.; Yung, K. H. *J. Phys. Chem.* **1995**, *99*, 12021.
(2) Garrido, J.; Linares-Solano, A.; Martin-Martinez, J. M.; Molina-Sabio, M.; Rodriguez-Reinoso, F.; Torregrosa, R. *Langmuir* **1987,** *3*, 76.
(3) Xing, B.; Pignatello, J. *Environ. Sci. Technol.* **1997**, *31*, 792.
(4) de Jonge, H.; Mittelmeier-Hezelejer, M. C. *Environ. Sci. Technol.* **1996**, *30*, 408.
(5) Dubinin, M. M.; Radushkevich, L. V. *Dokl. Akad. Nauk SSSR* **1948**, *55*, 331.
(6) Rodriguez-Reinoso, F.; Linares-Solano, A. In *Chemistry and Physics of Carbon*; Thrower, P. A., Ed.; Marcel Dekker: New York, 1998; Vol. 21, p 1.
(7) Cazorla-Amoros, D.; Alcaniz-Monge, J.; Linarez-Solano, A. *Langmuir* **1996**, *12*, 2820.
(8) Carrasco-Martin, F.; Lopez-Ramon, M. V.; Moreno-Castilla, C. *Langmuir* **1993**, *9*, 2758.
(9) Lamond, T. G.; Marsh, H. *Carbon* **1964**, *1*, 281.
(10) Guerin, H.; Siemieniewska, T.; Grillet, Y.; Francois, M. *Carbon* **1970**, *8*, 727.
(11) Walker, P. L.; Patel R. L. *Fuel* **1970**, *49*, 91.
(12) Bottani, E. J.; Bakaev, V.; Steele, W. A. *Chem. Eng. Sci.* **1994**, *49*, 2931.
(13) Bottani, E. J.; Ismail, M. K. I.; Bojan, M. J.; Steele, W. A. *Langmuir* **1994**, *10*, 3805.
(14) Cracknell, R. F.; Nicholson, D.; Tennison, S. R.; Bromhead, J. *Adsorption* **1996**, *2*, 193.
(15) Nicholson, D., Gubbins, K. E. *J. Chem. Phys.* **1996**, *104*, 8126.
(16) Nicholson, D. *Langmuir* **1999**, *15*, 2508.
(17) Gusev, V. Yu.; Neimark, A. V. In: *Extended Abstracts*, 23rd Biennal Conference on Carbon, Pennsylvania State University, 1997; p 64.
(18) Samios, S.; Stubos, A. K.; Kanellopoulos, N. K.; Cracknell, R. F.; Papadopoulos, G. K.; Nicholson, D. *Langmuir* **1997**, *13*, 2795.
(19) Ravikovitch, P. I.; Gusev, V. Yu.; Leon y Leon, C.; Neimark, A. V. In Extended Abstracts, 23rd Biennal Conference on Carbon, Pennsylvania State University, 1997; p 136.

10.1021/la990726c CCC: $18.00
Published on Web 09/23/1999

The simulation studies have shed light on maximum capacity of carbon pores for CO_2 sorption, molecular structure of CO_2 in pores, capillary condensation, and adsorption selectivity of some binary mixtures including CO_2. However, most of these works used different versions of the potential model of Hammonds et al.[20] for CO_2, which, to our knowledge, has never been shown to describe accurately vapor−liquid equilibrium in the bulk fluid. Deviations in the bulk saturation pressure and critical temperature may influence considerably the simulated adsorption isotherms. In particular, they lead to appreciable shifts in the capillary condensation pressures at low temperatures.

In the present paper we report a series of CO_2 isotherms in slit carbon pores at 273.2 K and pressures up to 1 atm, calculated using GCMC and NLDFT. The three-center representation of the CO_2 molecule due to Harris and Yung[1] was chosen to provide the best description of CO_2 bulk properties. Although less accurate for nonspherical molecules such as CO_2, NLDFT calculations have an advantage of being computationally much faster and easier to use, especially for pore characterization problems. We developed an effective Lennard-Jones (LJ) model for CO_2, which is used for calculations of adsorption isotherms. This model has been tested against the GCMC results for the three-center potential. GCMC simulations with an effective LJ model for CO_2 have also been performed for comparison.

2. Molecular Models

2.1 Fluid−Fluid Interactions. Three-Center GCMC Model. Several rigid three-center potential functions have been developed for CO_2 with interactions between the sites of different molecules modeled as a sum of LJ and electrostatic contributions:

$$U_{ij}(r) = 4\epsilon_{ij}\left[\left(\frac{\sigma_{ij}}{r}\right)^{12} - \left(\frac{\sigma_{ij}}{r}\right)^{6}\right] + \frac{q_i q_j}{r} \qquad (1)$$

where ϵ_{ij} and σ_{ij} are energetic and geometrical parameters of the LJ potential for sites i and j, and q_i and q_j are partial charges assigned to these sites to account for the quadrupole. For GCMC simulations we used the model of Harris and Yung,[1] which was shown to reproduce experimental densities of coexisting liquid and vapor phases and saturation pressure of the bulk[1,22] most accurately (Figure 1). Potential was cut at $r = 15$ Å and not shifted. However, when any two sites of two different molecules were inside the cutoff sphere, all nine site−site interactions for this pair of molecules were taken into account. Because quadrupole−quadrupole interactions decay as r^{-5}, considering relatively large cutoff and confinement, no long-range corrections were used. Parameters of the potential are shown in Table 1. The length of Markov chains in GCMC simulations was not less than 6×10^4 configurations per molecule; statistics were collected over ca. 3×10^4 configurations per molecule. The size of the GCMC simulation box was varied to ensure that sufficient number of particles remained in the simulation at each pressure.

Effective NLDFT Model. For NLDFT calculations, we applied an effective LJ representation of the CO_2 molecule. We used Tarazona's version of the NLDFT.[23]

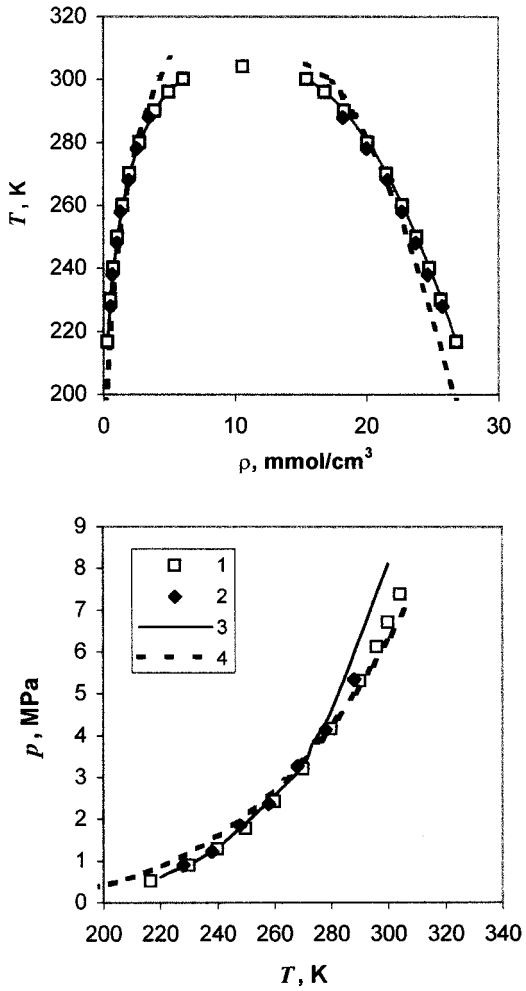

Figure 1. Densities of coexisting liquid and vapor phases (top) and saturation pressures (bottom) for bulk CO_2. 1, experimental data;[21] 2, results of Gibbs ensemble MC simulation[22] for three-center model of Harris and Yung;[1] 3, NLDFT model; 4, MC results for effective Lennard-Jones (LJ) fluid (calculated with equation of Johnson et al.[26]).

Table 1. Parameters of Intermolecular Potentials

three-center model			
ϵ_{O-O}/k, K	80.507	ϵ_{s-O}/k, K	47.563
σ_{O-O}, Å	3.033	σ_{s-O}, Å	3.217
ϵ_{C-C}/k, K	28.129	ϵ_{s-C}/k, K	3.107
σ_{C-C}, Å	2.757	σ_{s-C}, Å	28.13
ϵ_{C-O}/k, K	49.060	l_{O-O}, Å	2.232
σ_{C-O}, Å	2.892	q_O, a.u.	−0.3256

one-center model	GCMC	DFT
ϵ_{ff}/k, K	246.15	235.90
σ_{ff}, Å	3.6481	3.454
d_{HS}, Å		3.4947
ϵ_{sf}/k, K	81.49	81.49
σ_{sf}, Å	3.429	3.429

CO_2 is by no means a LJ fluid. However, it is still possible to describe interactions in the real system effectively, choosing LJ parameters and the hard-spheres diameter d_{HS} from the best fit of the DFT equation of state to the experimental liquid−vapor phase diagram. Using the WCA[24] prescription for attractive interactions and the cutoff of $5\sigma_{ff}$, we have obtained the parameters shown in Table 2. The LJ energy parameter ϵ_{ff} has to be temperature dependent, which reflects a strong contribution of qua-

(20) Hammonds, K. D.; McDonald, I. D.; Tildesley, D. J. *Mol. Phys.* **1993**, *78*, 173.

(21) Newitt, D. M.; Pai, M. U.; Kuloor, N. R.; Huggil, J. A. In *Thermodynamic Functions of Gases*; Din, F., Ed.; Butterworth: London, 1956; Vol. 123.

(22) Errington, J. Private communications; see http://thera.umd.edu/jerring/gibbs/results/co2_emp2/co2_emp2.html.

(23) Tarazona, P. *Phys. Rev. A* **1985**, *31*, 2672; errata *32*, 3148.

Table 2. Effective Lennard-Jones Representation of CO_2 at Different Temperatures[a]

T, K	220	240	260	273.15	280	300
ϵ_{ff}/k, K	275.69	258.81	244.57	235.94	231.46	215.49
d_{HS}, Å	3.5845	3.5547	3.5203	3.4947	3.4794	3.4179

[a] $\sigma_{ff} = 3.454$ Å.

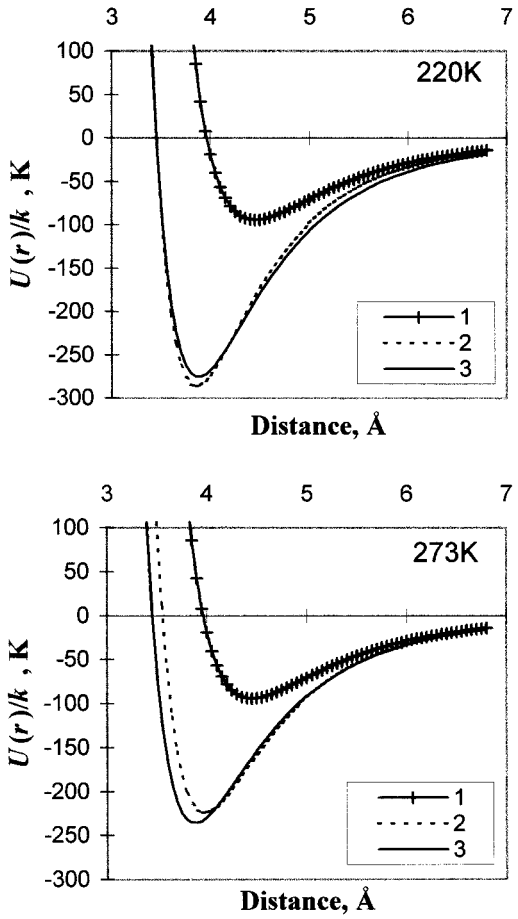

Figure 2. Effective representation of intermolecular interactions in bulk CO_2 with LJ potential. 1, dispersion LJ energy; 2, sum of the dispersion contribution and Boltzmann-weighted angle average of the quadrupole−quadrupole energy (eq 2); 3, effective LJ potential with parameters from Table 2. Top: T = 220 K; bottom: T = 273.2 K.

drupolar interactions. The liquid and vapor densities are predicted with accuracy of 0.5% in a wide range of temperatures; calculated saturation pressure at 273 K is ca. 8% higher compared with the experimental (Figure 1). The LJ parameters for 273.2 K are also given in Table 1.

The use of the temperature-dependent LJ parameters can be justified from the following. Consider a model in which interactions between CO_2 molecules are approximated with a temperature-independent LJ dispersion term plus the Boltzmann-weighted angle average of the quadrupole−quadrupole energy:[25]

$$U(r) = 4\epsilon_{disp}\left[\left(\frac{\sigma_{disp}}{r}\right)^{12} - \left(\frac{\sigma_{disp}}{r}\right)^{6}\right] - \frac{14\Theta^4}{5r^{10}k_B T(4\pi\epsilon_0)^2} \quad (2)$$

where $\Theta = -14.9 \times 10^{-40}$ C m^2 (ref 25) is the quadrupole moment of the CO_2 molecule. As displayed in Figure 2, this potential field can be approximated by the effective LJ potential with temperature-dependent parameters determined by fitting to the bulk properties. The parameters of the dispersion term in eq 2 were estimated as: $\epsilon_{disp}/k = 94.38$ K and $\sigma_{disp} = 3.963$ Å.

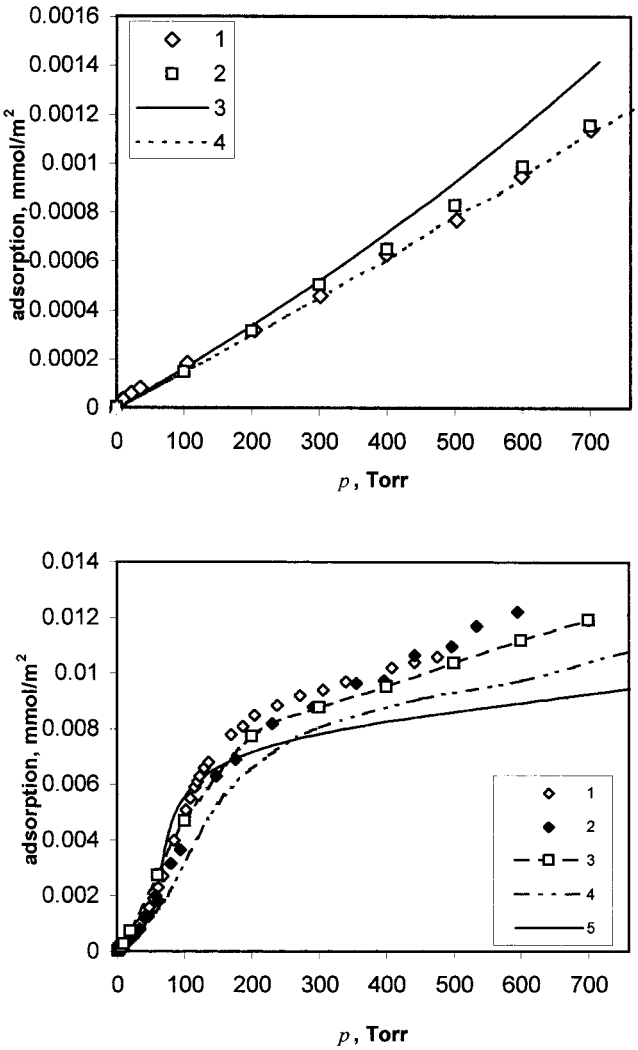

Figure 3. Simulated isotherms compared with experimental data for CO_2 adsorption on graphitized carbon blacks. Top: T = 273.2 K. 1, experimental data of Bottani et al.;[12,13] 2, MC results for the three-center model; 3, DFT results; 4, MC results for the effective LJ fluid. Bottom: T = 195.5 K 1, experimental data of Beebe et al. for CO_2 (Sterling graphite at 193.2 K[29]); 2, experimental of Bottani et al.;[12] 3, GCMC results for three-center model of Harris and Yung;[1] 4, NLDFT results; 5, GCMC results for the effective LJ fluid.

One-Center GCMC Model. For comparison, we have also performed a series of GCMC simulations with a one-center LJ model for CO_2. A comprehensive comparison of DFT and MC approaches is beyond the scope of this paper; however, it should be noted that it is not appropriate to use LJ parameters obtained for DFT in MC simulations. The models are consistent only when both of them provide a correct description of bulk equilibrium. Therefore, the LJ parameters were estimated from the fit of the equation of state for LJ fluid of Johnson et al.[26] to experimental data at a single temperature 273 K (Figure 1). The potential was cut at 5σ and not shifted. Parameters of this LJ model are also shown in Table 1.

(24) Weeks, J. D.; Chandler, D.; Andersen, H. C. *J. Chem. Phys.* **1971**, *54*, 5237.

(25) Rigby, M.; Smith, E. B.; Wakeham, W. A.; Maitland, G. C. *The Forces Between Molecules*; Clarendon Press: Oxford, 1986; p. 8.

(26) Johnson, J. K.; Zollweg, J. A.; Gubbins, K. E. *Mol. Phys.* **1993**, *78*, 591.

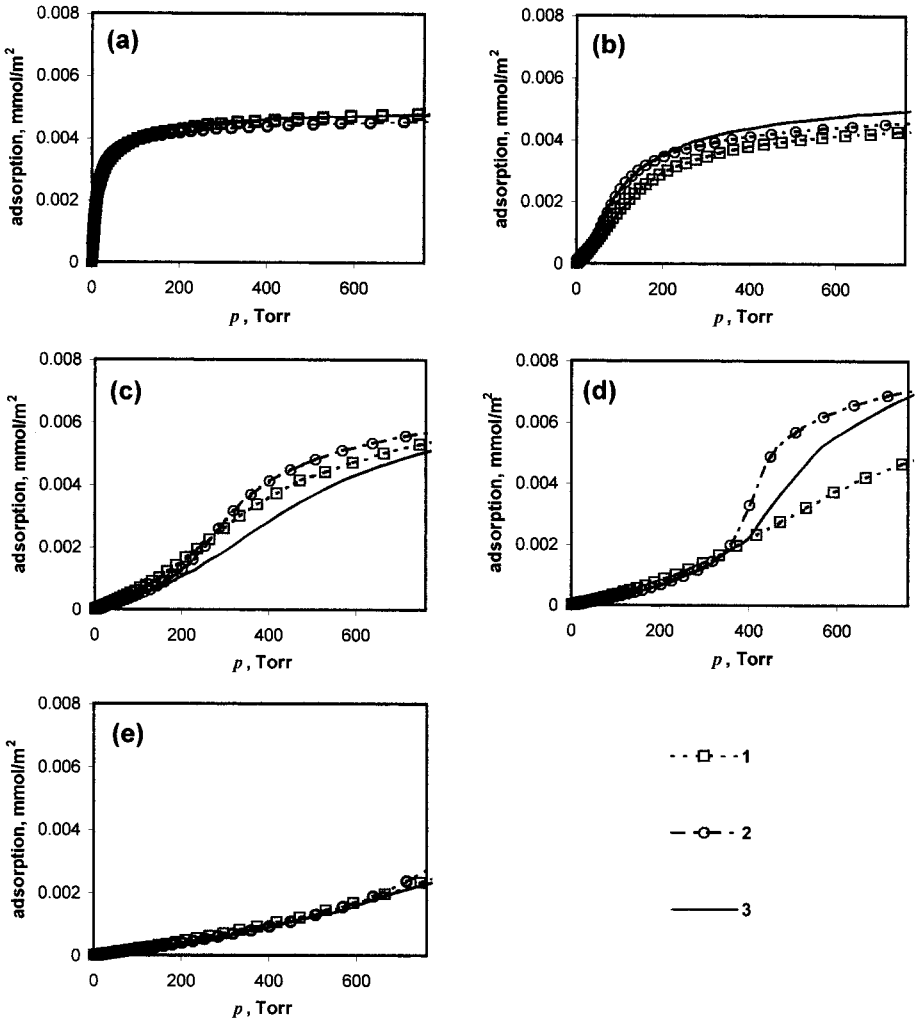

Figure 4. Adsorption isotherms in individual slit pores at 273.2 K. 1, GCMC results for the three-center model of Harris and Yung,[1] 2, NLDFT results; 3, GCMC results for effective LJ fluid. $h = 3.65$ Å (a); $h = 5.01$ Å (b); $h = 6.27$ Å (c); $h = 7.18$ Å (d); $h = 8.99$ Å (e).

2.2 Solid−Fluid Interactions. In accord with standard representation, carbon micropores were considered as slit-shaped. The carbon surface was treated as graphite-type stacked planes of carbon atoms. The interaction between each site of an adsorbate and a graphite surface is given by the 10−4−3 potential of Steele:[27]

$$U_{sf}(z) = 2\pi\rho_s\epsilon_{si}\sigma_{si}^2\Delta\left[\left(\frac{\sigma_{si}}{z}\right)^{10} - \left(\frac{\sigma_{si}}{z}\right)^4 - \frac{\sigma_{si}^4}{3\Delta(0.61\Delta + z)^3}\right] \quad (3)$$

where Δ is the separation between layers in graphite, ρ_s is the number density of carbon atoms in graphite, z is the distance from the site of a fluid molecule to the nuclei of the carbon atoms in the surface graphitic plane, ϵ_{si} and σ_{si} are the LJ parameters for site i and the graphite carbon atom. The total solid−fluid potential is given by:

$$U_{sf}^{(\text{total})} = U_{sf}(z) + U_{sf}(H - z) \quad (4)$$

where H is the distance between the nuclei of carbon atoms on opposite walls. The internal pore width h, which is determined experimentally, can be calculated as $h = H - \sigma_s$, where σ_s is the LJ diameter of the carbon atom. The simplest way of parametrization of the 10−4−3 potential is to apply the Lorentz−Berthelot rules for each site of the fluid molecule, using the values $\epsilon_s/k = 28.1$ K and $\sigma_s = 3.4$ Å for carbon−carbon interactions in graphite.[27] However, this approach is not accurate enough even for noble gases.[28] We have determined the solid−fluid parameters by fitting the simulated adsorption isotherm on an open carbon surface to the reference experimental isotherm of CO_2 on graphite. For this purpose we analyzed a number of adsorption isotherms for CO_2 on several graphitized carbon blacks at 273.15 K and $p < 1$ atm. At these conditions the isotherms are almost linear; the difference between the slopes of different isotherms is up to 20%, mostly due to uncertainties in determining the surface area of different samples by the BET method. We used data of Bottani et al.[12] as a reference (Figure 3); the values of σ_{si} were obtained using Lorentz−Berthelot rules assuming $\sigma_c = 3.4$ Å, and the values of ϵ_{si} were fitted to reproduce the reference isotherm. This procedure was applied to determine the solid−fluid parameters for all three models. All solid−fluid parameters are listed in Table 1. The values of ϵ_{sj}, obtained for carbon and oxygen atoms of the three-center model of the CO_2 molecule, are 4.4% higher compared to those estimated with the combination rules; however, this minor difference is essential and leads to roughly a 23% increase in slope of the adsorption

(27) Steele, W. A. *The Interactions of Gases with Solid Surfaces*; Pergamon: Oxford, 1974.

(28) Steele, W. A. *J. Phys. Chem.* **1978**, *82*, 817.

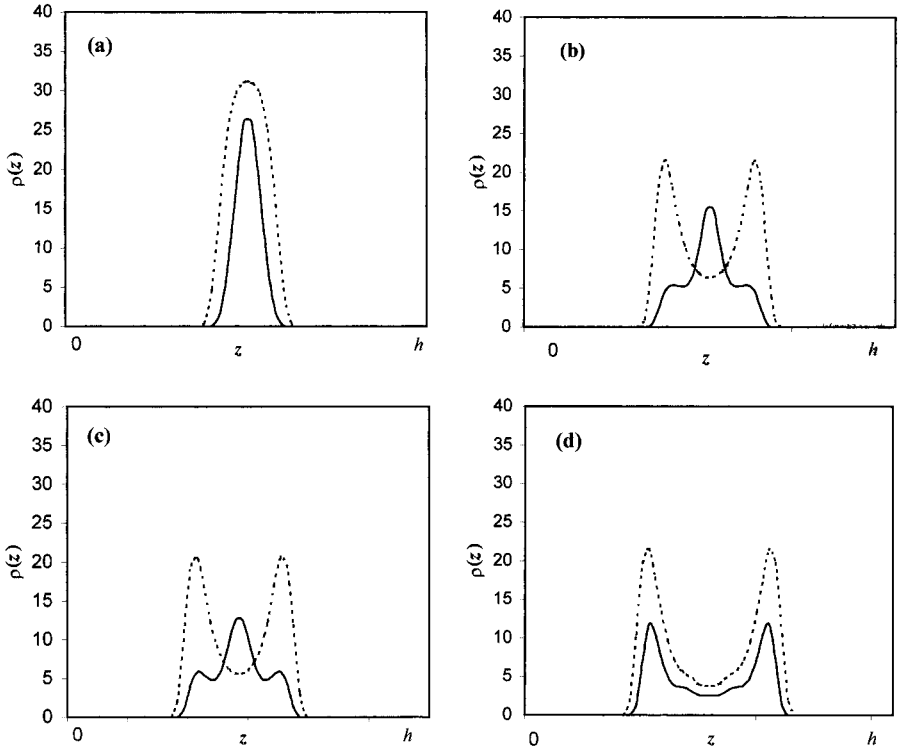

Figure 5. Local density profiles for carbons (solid line) and oxygens (dashed line) of CO_2 in slit carbon pores at 273.2 K and 1 atm, calculated with the three-center model using GCMC method. $h = 3.65$ Å (a); $h = 5.01$ Å (b); $h = 5.24$ Å (c); $h = 6.27$ Å (d).

isotherm. The calculated value of ϵ_{sf} for the DFT LJ model practically coincides with the combination rule estimate; for the MC LJ model the combination rule gives ca. 2% higher value.

Calculated adsorption isotherms at $T = 273.15$ K are shown in Figure 3 (top). The second virial coefficients for all three models are practically equal, but the isotherm calculated using DFT is substantially nonlinear, which causes deviations from the experiment and MC results at higher pressures. However, these deviations are still of the same order as the experimental uncertainty. To verify fluid−fluid and solid−fluid parameters, adsorption isotherms at CO_2 boiling temperature $T = 195.5$ K, at which the adsorbate forms a condensed monolayer, were calculated. Both simulated and experimental isotherms[12,29] are shown in Figure 3 (bottom). The agreement between the experimental isotherms and the calculated isotherm for the three-center model is very good for both temperatures. For the LJ representations of the adsorbate the agreement is poorer, yet satisfactory.

3. Results and Discussion

Using the GCMC and NLDFT methods we calculated a series of adsorption isotherms in pores of $h = 2.6-15$ Å at $T = 273.15$ K and $p < 1$ atm. The pores with $h < 2.6$ Å are too narrow and do not adsorb CO_2 at these conditions. As the pore width increases up to 3 Å, the CO_2 forms a dense monolayer. For the three-center model in graphite pores the second virial coefficient goes through a maximum at $h \approx 3.15$ Å. Because the LJ representations of CO_2 assume a larger molecular diameter than σ_{O-O}, the maximum of the second virial coefficient for these models is achieved in wider pores, $h \approx 3.65$ Å. However, even the pores corresponding to the maximum of the second virial coefficient are filled at $p > 3 \times 10^{-3}$atm, that is, within the range of pressures easily accessible experimentally. This is a considerable advantage of using CO_2 for carbon characterization. In these narrow pores, adsorption isotherms for all three models show quite good agreement, in favor of the less computationally expensive DFT approach (Figure 4a).

The molecular structure of the adsorbate is demonstrated by local density profiles. In the case of the three-center model, the density profiles can be calculated separately for carbon and oxygen atoms (Figure 5), providing information on the predominant orientation of CO_2 molecules with respect to the pore walls. Detailed analysis of the adsorbate structure can be based on the density orientation distribution:

$$\rho(z,\theta) = \mathrm{d}N(z,\theta)/\mathrm{d}z \sin\theta \mathrm{d}\theta \qquad (5)$$

Here, $\mathrm{d}N(z,\theta)$ is the number of molecules whose center of mass is located at the distance $z \div z + \mathrm{d}z$ to the nearest wall and molecular axis forms angle θ to the normal to the walls; $\theta = \pi/2$ corresponds to the parallel orientation toward the walls, $\theta = 0$ and $\theta = \pi$ correspond to the normal orientation. In other works[14,18] the orientational structure of the CO_2 molecules in pores was studied on the basis of the mean square cosine between the molecular axis and the normal to the walls. At $h < 4$ Å the CO_2 molecules are oriented strictly parallel to the walls, as the pore space is insufficient for perpendicular orientation. It should be noted that the CO_2 molecule is energetically favored to lie flat on the wall at any pore width, because all three atoms of the molecule are in the potential minimum. However, as the pore width increases, the dependence of the adsorption energy on θ becomes bimodal, with the secondary minimum corresponding to a slanted orientation toward the walls. In this case, both oxygen atoms are in their potential minima near different walls of the pore, whereas the carbon atom is located in the energetically unfavorable position in the middle of the pore. The second minimum of the adsorption energy disappears as soon as

(29) Beebe, R. A.; Kiselev, A. V.; Kovaleva, N. V.; Tyson, R. F. S.; Holmes, J. M. *Russ. J. Phys. Chem. (Transl. of Zh. Fiz. Khim.)* **1964**, *38*, 372.

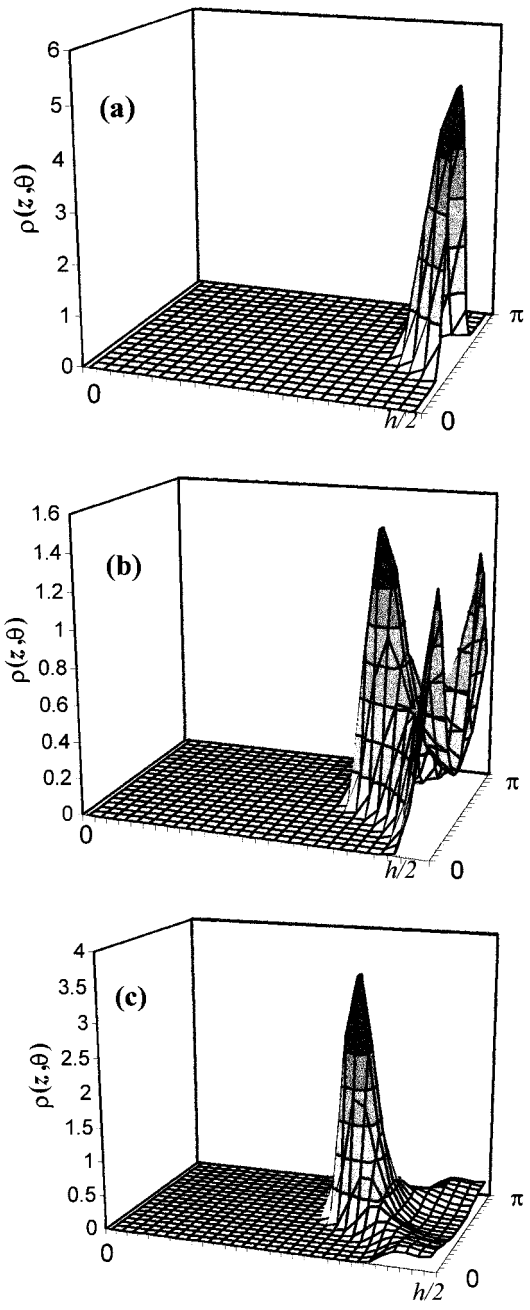

Figure 6. Density orientation profiles for CO_2 in slit carbon pores at 273.2 K and 1 atm. $h = 3.65$ Å (a); $h = 5.01$ Å (b); $h = 6.27$ Å (c).

the pore width becomes considerably larger than the length of the CO_2 molecule. Orientation structure of the adsorbate changes correspondingly. Figures 5a and 6a show that at $h = 3.65$ Å the alignment parallel to the walls is highly preferential. As the pore width increases, the density orientation distribution becomes bimodal. At low densities the CO_2 molecules are still mostly oriented parallel with respect to the walls. However, the situation changes when the fluid density in the pore is considerable and the fluid−fluid interactions contribute substantially to the total potential energy. As shown in Figure 5b, for $h = 5.01$ Å at $p = 1$ atm two distinct submonolayers of the fluid molecules, parallel and slanted toward the walls, are observed. The local density profiles (Figure 5b) show that the slanted orientation is preferential at these conditions: the density profiles for the carbon atoms still show one-layer structure, whereas density profiles of oxygens become bimodal. Molecules with the slanted orientation show preference to the X-like configuration with respect to each other and to distorted T-like configuration with the molecules oriented parallel to the walls. Because of the strong electrostatic contribution to the fluid−fluid potential energy, the orientation normal to the walls never becomes predominant for CO_2, as in this case molecules would have to align parallel to each other. In contrast to diatomic fluids,[30] CO_2 molecules still prefer the slanted alignment, then start to form a two-layer structure even when the secondary minimum of the adsorption potential corresponds to the normal orientation ($h = 5.24$ Å, Figure 5c). At $h = 6.27$ Å, two distinct layers parallel to the pore walls are formed (Figures 5d, 6c).

The structure of the LJ fluid in these pores is, of course, quite different from that for the three-center model; its dependence on the pore width exhibits all typical features described in the literature. However, the adsorption isotherms for all three models are still in reasonable agreement (Figure 4b, c). For the purpose of pore characterization, the most important parameters are the pressure range, corresponding to the pore filling, and the total density of the adsorbate when the pore is filled. Both of these parameters are reproduced with a reasonable accuracy with the LJ models for $h \leq 6.27$ Å, despite a larger second virial coefficient for the three-center fluid (Figure 4c). Substantial discrepancies between the isotherms for the three-center and LJ models appear as soon as the LJ fluid undergoes a transition to pronounced two-layer structure. This transition, which is always observed for a LJ fluid in idealized slit-shaped pores, is supposed to be responsible for artificial minimum on pore size distributions at $h \approx 1.6-1.8\sigma_{ff}$, similar to that recently reported by Olivier for nitrogen and argon adsorption.[31] Compared with spherical LJ molecules, the three-center CO_2 provides much lower density in the two-layer state at $p = 1$ atm, despite having a larger second virial coefficient (Figure 4d). The density of the adsorbate in the two-layer state at atmospheric pressure exceeds that in the monolayer state by only 20% (Figure 4a, d). We assume that this effect is also due to the electrostatic contribution to the fluid-fluid potential energy. Bulk quadrupolar liquids are known to have a rather complex structure. The structure of a confined fluid is quite different. In the pore of $h \approx 7$ Å the three-center CO_2 molecules must align strictly parallel to the walls. In each of the monolayers CO_2 molecules give preference to a T-like alignment toward each other. At the same time, the molecules from different layers should prefer an X-like or a distorted T-like alignment. Apparently, these two tendencies are contradicting. To check this assumption, we performed a single simulation with the three-center CO_2 model in the pore $h = 7$ Å at $p = 1$ atm, where two dense monolayers are formed, and evaluated different contributions to fluid-fluid potential energy. The contribution of electrostatic interactions was only 24%, compared with 35% in the monolayer and 39% in the bulk.

Because the transition to a three-layer structure lies outside the pressure range under consideration, the adsorption is gets lower with a further increase in pore width and the shape of the isotherms becomes closer to linear for all three models. The molecules are oriented parallel to the walls, and the agreement between LJ and three-center models gets better (Figure 4e). At $h \geq 10$ Å we observe just monolayer adsorption of CO_2 on each of the pore walls, confirming the assumption made in refs

(30) Klochko, A. V.; Piotrovskaya, E. M.; Brodskaya, E. N. *Langmuir* **1999**, *15*, 545.
(31) Olivier, J. P. *Carbon* **1998**, *36*, 1469.

9 and 10. The isotherms have no unique features and are linearly dependent. This defines the upper limit of sensitivity for the pore characterization method, on the basis of CO_2 adsorption at ambient conditions. We estimate that only ultramicroporous carbon adsorbents, containing pores narrower than ~9 Å, are efficient for CO_2 sorption at ambient conditions. By the same reasons, only pores narrower than 9−10 Å can be probed by CO_2. To characterize wider pores by CO_2 sorption at 273 K, pressures greater than 1 atm should be considered. High-pressure adsorption measurements have been successfully applied for characterization of porous structure of activated carbons.[7] The NLDFT model for high-pressure CO_2 adsorption in carbon pores and based on this model method for pore size analysis will be presented elsewhere.[32]

4. Conclusion

We have calculated a series of adsorption isotherms in individual slit-shaped carbon pores at $T = 273$ K and $p < 1$ atm using the GCMC method and the NLDFT. In GCMC the CO_2 molecule was presented by the three-center model. In NLDFT the effective LJ parameters have been determined to reproduce with the best possible accuracy the experimental data for vapor−liquid equilibrium in the vicinity of 273 K. Parametrization of the adsorption potential was based on experimental data on CO_2 adsorption on nonporous graphite at the same temperature. This parametrization also provides a good agreement between simulated and experimental adsorption isotherms at the CO_2 boiling temperature195.5 K.

It is shown that the CO_2 molecules form a dense monolayer in pores wider than 3 Å. These pores are filled by the adsorbate at $p \approx 5 \times 10^{-3}$ atm, which is easily measured experimentally. This means that even the most narrow pores can be characterized with CO_2 adsorption at 273 K. As the pore width increases in the range $6.5 \geq h \geq 8$ Å, the adsorbate undergoes a transition from a one-layer to a two-layer structure. In wider pores, the CO_2 molecules form two monolayers on the opposite pore walls. The central part of these pores remains unfilled at subatmospheric pressures. This determines 9−10 Å as the upper limit of sensitivity of subatmospheric CO_2 adsorption at 273 K to the pore sizes.

For pores narrower than 6.5 Å and wider than 9 Å, the isotherms calculated by the NLDFT model, are in a good agreement with the isotherms obtained by the three-center GCMC simulation. In the range $6.5 \geq h \geq 8$ Å, where the adsorbate undergoes a transition from a one-layer to a two-layer structure, the discrepancies are significant. The GCMC results for the LJ CO_2 model agree well with NLDFT predictions for all pore widths, indicating that the above-mentioned discrepancies are due to shortcomings of the spherical representation of the CO_2 molecule, rather than to the meanfield nature of the NLDFT approach. The models developed in the present work can be used for the prediction of CO_2 sorption by nanoporous sorbents and for the quantitative characterization of nanoporosity in carbonaceous materials, including coals and soil particles.

Acknowledgment. This work has been supported in parts by EPA grant R825959-010 and by Quantachrome Corporation.

LA990726C

(32) Ravikovitch, P. I.; Vishnyakov, A.; Russo, R.; Neimark, A. V. *Langmuir*, submitted for publication.